

Heat Load Problems on Storage Ring Vacuum Chambers at ELETTRA

A. Gambitta, A. Turchet

*Sincrotrone Trieste, in Area Science Park, S.S. 14 Km 163.5, 34012 Trieste, Italy
Phone: + 39 - (0) 40 - 3758676; Fax: + 39 - (0) 40 - 3758565
E-mail: alessandro.gambitta@elettra.trieste.it*

Abstract

The ELETTRA storage ring, in operation since October 1993, was originally designed with all its vacuum chambers in AISI 316 LN stainless steel. New beamline projects have required the development of new kinds of insertion devices (ID) that can work in circular and vertical polarized modes besides the usual linear one. These new ID working modes however have undesirable heat load effects on the bending magnet vacuum chambers. For this reason new chambers have been developed in aluminum alloy, because of the higher value of thermal conductivity, with internal water-cooling channels close to the critical points of interaction with the photon beam. In this paper we describe some aspects of the aluminum chamber activities, focusing our attention on heat load problems.

Keywords: aluminum chambers, heat load, undulators

1. Introduction

The original project of the ELETTRA storage ring was planned with two families of bending magnet vacuum chambers. Twelve identical chambers were made for the bending magnet exit ports; eleven identical chambers were mounted for the insertion device (ID) exit ports and a hybrid chamber after the injection section. The material used for all of these chambers is AISI 316 LN stainless steel that has low magnetic permeability ($\mu < 1.007$) and proved vacuum compatibility, but low thermal conductivity.

The recent developments for the ELETTRA beamlines have required the installation of variable polarization undulators of the APPLE II type. The beamlines with these ID sources are the Nanospectroscopy, the Advanced Photoelectric-effect Experiments (APE) and the Beamline for Advanced DiChroism (BACH). The experiments in these beamlines require circular and in several cases vertical polarized modes from the ID. The shape of the photon beam in these modes, as shown in the following, interferes with the internal slots of the chambers and therefore an efficient cooling system had to be considered.

This is one of the major reasons to develop the new vacuum chambers for the exit ports of these beamlines with internal cooling channels and aluminum alloy, which is about 10-times better in thermal conductivity than stainless steel. The choice of aluminum alloy has also been made to improve the cooling efficiency of the chambers downstream the photon absorber and unshielded by the absorber itself, which in the previous stainless steel chambers has been recognized as a critical point.

2. Some Aspects of Aluminum Chamber Project

The manufacturing of the chamber has been made by machining top and bottom shells. These have been welded together throughout the symmetry plane. The whole process has been carefully studied and tested before the final assembly by our Quality Control Group. The material of the chamber body is the alloy ASTM B209 Al 5083 [1,2] which has good technological characteristics (welding, machining) and mechanical behavior in the temper H321 (minimum yield strength 200 MPa, minimum tensile strength 285 MPa).

In Fig. 1 the top shell of the chamber is visible during machining of the internal part in which one can see one half of the rhomboidal chamber (right side, close to the milling machine) of the electron beam as it deflects 15° in the horizontal plane. On the left side, one half of the rectangular photon beam exit port is visible. In the white box is shown the possible point of interaction of the photon beam with the rhomboidal wall of the chamber.



Fig. 1: Chamber machining.

Particular care has been taken for the internal roughness that has been limited to a maximum value of $0.2\text{-}0.4\ \mu\text{m rms}$ for vacuum purposes. In general the design of the chamber is more compact with respect to the older stainless steel chamber in order to minimize the deformation due to the lower Young modulus and in any case to limit the maximum stresses in the welded joint.

Figure 2 shows a 3D CAD model of the chamber assembly with all its flanges and the cooling pipes. On the left side the aluminum straight pipe is visible, welded to the chamber body in a second step and constituting the exit pipe for the electrons. This pipe is made by an extrusion of aluminum alloy 6061 [3] and includes an internal cooling channel because the photon absorber cannot shade this part of the chamber from the bending magnet photon beam. On the bottom side the pumping flange is visible, in front

of the flange with the rectangular slot is the photon beam exit, while on the right side the flange for the photon absorber insertion is shown.

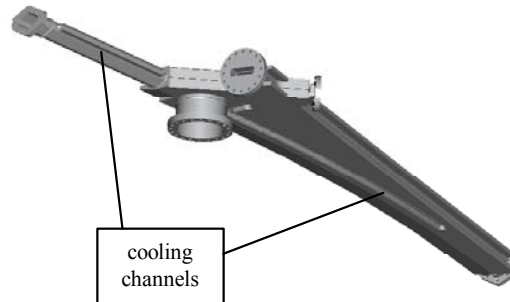


Fig. 2: 3D drawing of the chamber.

All of the flanges are in aluminum alloy and must be connected to the existing stainless steel flanges, therefore soft special gaskets of pure Aluminum (99.5%) have been used for the connection; the cross section of the gasket is diamond shaped and the seal is realized by deforming the gasket edges with the planar surface of the two flanges.

3. Heat Load Problems

In the vacuum chamber there are three major zones that can be critical from the thermal point of view. The first zone is outlined by the white box of Fig. 1 in which the photon beam produced from the undulator leaves the rhomboidal chamber of the electron beam through the appropriate chamber slots. In Fig. 3 a cross section of the chamber in the mentioned zone is shown in which is qualitatively sketched two possible shapes of the ID photon beam; the elliptical one is relative to the linear polarization mode of the undulator and is the usual mode in which the photon beam does not interfere with the chambers walls, while the second is relative to a circular polarization mode.

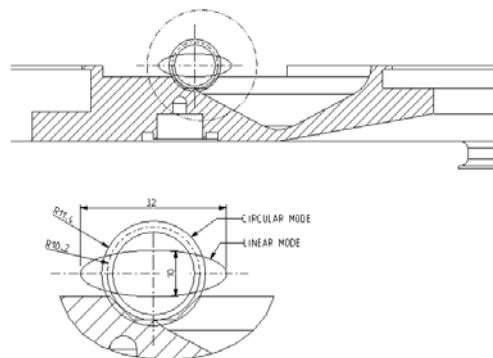


Fig. 3: Cross section of the chamber in the critical zone.

In general we can say that, for certain fixed machine parameters (i.e. energy, current), the dimensions of the two shapes increase when the gap of the undulator is decreasing, corresponding to lower photon energies. However, while in the linear polarization mode the beam extends only in the horizontal direction, and therefore does not interfere with the chamber, in circular polarization mode the radius increases (the solid angle of the cone) and therefore can hit the chamber wall; moreover the maximum power density is concentrated at the external radius of the beam. The vertical polarization mode is the same shape as the linear one, but rotated by 90°. Decreasing the undulator gap could result in the photon beam being intercepted by the chamber.

The results of the finite element calculation of this zone will be discussed in the next section in which the behavior of the FEL-Nanospectroscopy chamber heated by the photon beam will be considered in the worst cases of circular and vertical polarization modes. This chamber has been recognized has the most critical among the new ones.

The other two critical zones from the heat load point of view can be considered more “conventional” because they are the ones heated by the bending magnet radiation. Other than the few mrad accepted by the beamline the major part of this radiation is taken by the photon absorber that protects the end wall of the chamber from heating, but cannot shadow the exit pipe, which therefore includes in the extrusion an appropriate channel for the cooling.

4. The FEM Model

In this section the results of a finite element model are presented, which describe two extreme load cases in circular and vertical polarization mode for the elliptical undulators EU10.0 that serve the Fel-Nanospectroscopy beamlines.

These cases are considered as extreme because they arise from the undulators being set at the minimum gap in the two modes, which is not necessarily an operational requirement of the beamlines.

In Fig. 4 the power density distribution [4] is shown in the two modes with the machine at 2 GeV and 400 mA projected at the slot. To be noticed, as an example, that the beamline FEL will always operate at 1 GeV, while for the Nanospectroscopy the required photon energies comes from higher values of the gap and therefore lower load cases.

In the case of circular polarization the abscissa is the radius in the direction normal to the beam axis and the total power is 3737 W, while the peak power density is 24.3 W/mm²; these values were fitted from the original data in angular distribution with the software Mathematica and then calculated for the average distance from the source in the struck zone that is 6154 mm. In the vertical polarization mode the total power is 4683 W and the maximum power density is 77.6 W/mm² in the plane normal to the beam axis; in this case the abscissa is the vertical axis for the parabolic distribution and the horizontal one for the Gaussian distribution.

The two power distributions have been simplified in both cases to be applied more easily to the model. The circular case has been described as a constant distribution over a ring in which the average radius is relative to the maximum power density in the true case; the width of the ring is selected in such a way that the total power is the same as in the real distribution.

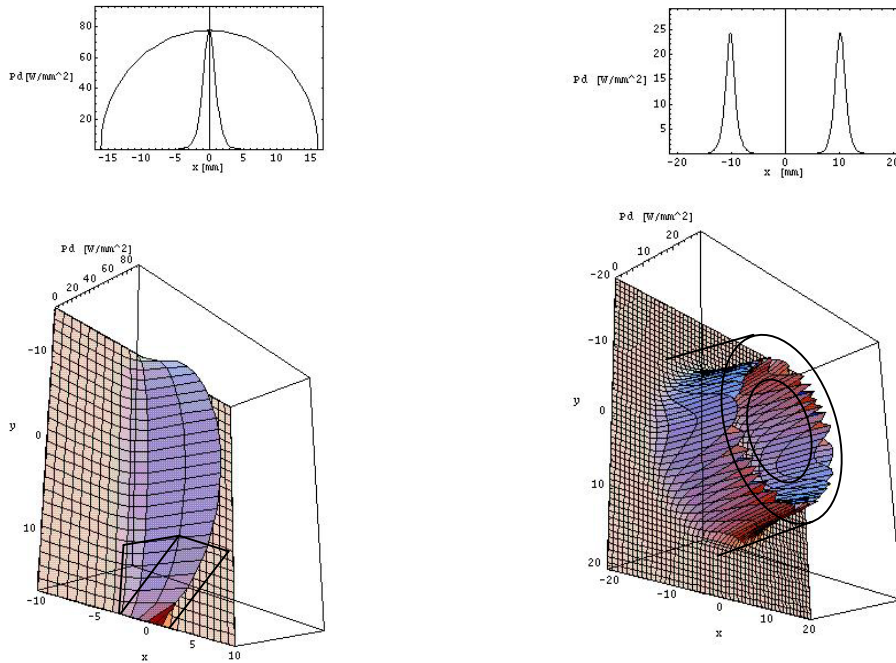


Fig. 4: Power density distribution.

In the vertical mode the beam could strike the chamber with the end part of the vertical distribution of the beam that has been simplified as a triangular distribution in y axis and constant in x axis (Fig. 4).

The model of the chamber has been done using the CAD program Pro-Engineer, and the same program used to determine the surfaces of interaction with the beam. In Fig. 5 we can see, as an example, the surfaces of intersection in a 3D model in the case of circular polarization. It has to be noted that only a small part of the total power is absorbed by the chamber (630 W in the circular mode and 611 W in vertical mode); moreover the power is absorbed with an incidence angle with the normal plane that is, on an average, 7° and therefore the maximum power densities are not so high (3.2 W/mm^2 in the circular mode and 4.8 W/mm^2 in vertical mode).

A meaningful sub-assembly of the chamber has been pre-processed using the program Patran that has been used to simplify the geometry, meshing the model with tetrahedral elements with 10 nodes, loading the power density mentioned before, fixing the film coefficient inside the water channel, giving the material properties and so on. As a result of this phase we got input files for the finite element solver that in our case is the Abaqus software.

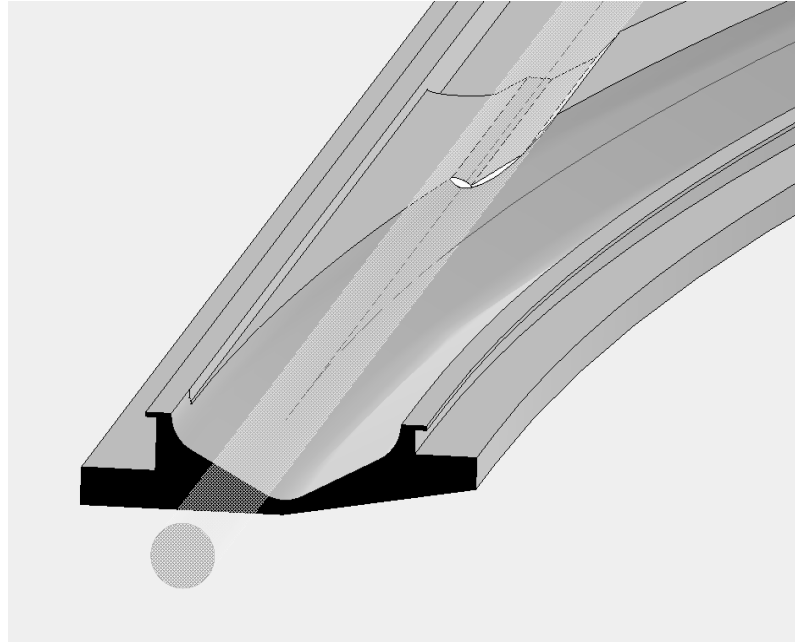


Fig. 5: Surfaces of intersection with the beam.

The film coefficient was calculated using the Dittus-Boelter formula [5], assuming a water flux of 5.1 l/min inside the cooling channel having an equivalent diameter of 5.5 mm. The resulting value of the film coefficient is $h=12900$ W/mK.

The results of the two calculations are shown in Fig. 6 and Fig. 7 for the circular and vertical polarization modes respectively.

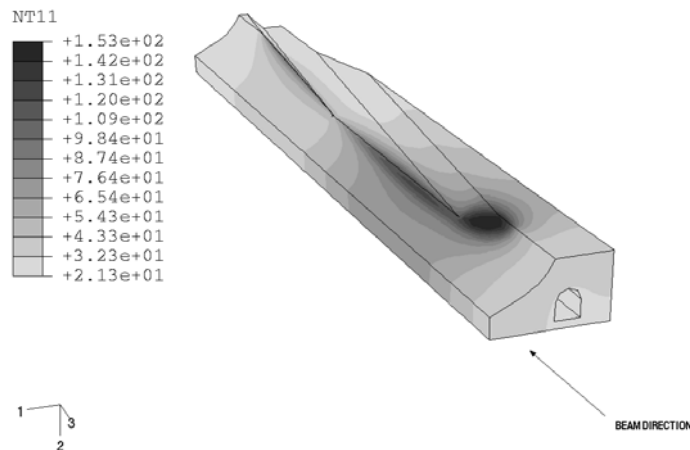


Fig. 6: FEM analysis of circular polarization mode.

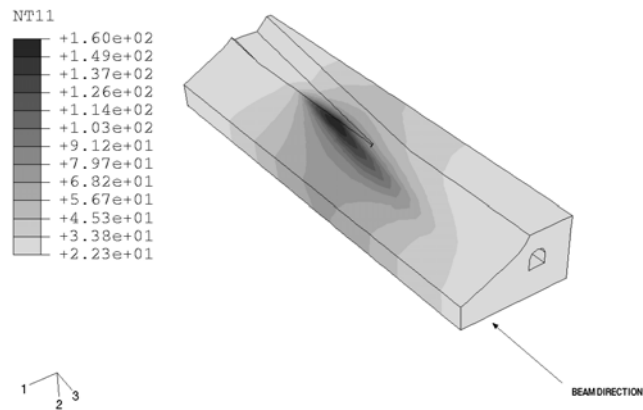


Fig.7: FEM analysis of vertical polarization mode.

The temperature fields resulting by the analysis of the two modes is reported in Fig. 6 and Fig. 7. In Table 1 is then summarized the maximum temperature on the surface of the inside channel (T_{ch}) and the maximum temperature on the slot (T_{max}).

Table 1: Maximum Temperatures for the Two Modes

	T_{ch} [°C]	T_{max} [°C]
Circular Polarization Mode	74	153
Vertical Polarization Mode	77	160

5. Conclusions

The calculation has shown good thermal behavior of the aluminum chamber, the maximum temperature is quite high but reasonable and incipient boiling inside the cooling channel does not occur. It has to be underlined that the maximum heat loads are not working conditions but those maximum achievable with the undulators at the minimum gap. In reality the gap of undulators will be limited for each polarization mode to more reasonable values. Moreover there are two thermocouples close to the critical points with which we can control the true behavior of the chamber in all that cases that are difficult to study beforehand (as an example misalignment).

6. Acknowledgments

The aluminum chamber project is the result of the work of many people under the responsibility of N. Pangos for the overall project. In particular the authors wish to thank B. Diviacco for the power distribution calculations, and C. Fava and G. Loda for technical support.

7. References

- [1] N. Pangos, “Prescrizioni di Fornitura per la Fabbricazione di Camere da Ultra Alto Vuoto in Alluminio,” Specifica Tecnica Generale SG113, Sincrotrone Trieste, Italy, April 1998.
- [2] V. Chimenti, Y. He, H. Hsieh, V. Lollo, “Specification for Storage Ring Arc Vacuum Chamber DaFne Project,” Specification n.SR-02.35-SP01-4-A, INFN Frascati, Italy, March 1994.
- [3] J. R. Noonan, J. Gagliano, G. A. Goepfner, R. A. Rosenberg, D. R. Walters, “APS Storage Ring Vacuum System Performances,” 1997 Particle Accelerator Conference, Vancouver, May 1998, pp.3552-3555.
- [4] B. Diviaco, private communication.
- [5] V. M. Rohsenow, J. P. Hartnett, E. N. Ganic, Handbook of Heat Transfer Fundamentals, McGraw-Hill, New York, 1985.